TECHNICAL NOTES

NATIONAL ADVISORY COMMITTEE FOR AERONAUTICS

No. 511

A STUDY OF THE PITCHING MOMENTS AND
THE STABILITY CHARACTERISTICS OF MONOPLANES

By George J. Higgins

Washington
November 1934

NATIONAL ADVISORY COMMITTEE FOR AERONAUTICS

TECHNICAL NOTE NO. 511

A STUDY OF THE PITCHING MOMENTS AND

THE STABILITY CHARACTERISTICS OF MONOPLANES*

By George J. Higgins

SUMMARY

This note presents a study of the pitching moments and the stability characteristics of monoplanes. Expressions for the pitching-moment coefficient and the Diehl stability coefficient for the monoplane are developed, suitable for the use of airplane designers. The effective difference between the high-wing and low-wing types is portrayed and discussed. Comparisons between experimental and computed values are made. Charts for use in the solution of numerical values of the pitching-moment and stability coefficients are presented.

NOTATION OF SYMBOLS

The basic symbols are used alone and also with subscripts, w for wing and t for tail; e.g., S_w, wing area and C_{L_t}, lift coefficient of tail.

M, pitching moment, ft.-lb.

$M_{c.g.}$, pitching moment about the center of gravity.

$M_{0.24c}$, pitching moment about a point 24 percent of the chord from the leading edge on the mean aerodynamic chord.

$C_m = \dfrac{M}{qSc}$, pitching-moment coefficient.

---

*Thesis submitted in partial fulfillment of the requirements for the degree of Aeronautical Engineer in the Graduate School of the University of Michigan, June 1934.

S,   area.

c,   chord.

$q = \frac{1}{2} \rho \, V^2$, dynamic pressure, lb. per sq.ft.

ρ,   mass density of standard air, 0.002378 slugs
          per cu.ft. at 29.92 inches of Hg and 59° F.

V,   velocity, ft. per sec.

M.A.C.,   mean aerodynamic chord.

W,   weight, lb.

L,   lift, lb.

$C_L = \frac{L}{qS}$,   lift coefficient.

D,   drag, lb.

D_i,   induced drag.

D_o,   profile drag.

D_p,   parasite drag.

$C_D = \frac{D}{q\,S}$.

l,   lever arm of tail force, ft.

η,   tail efficiency.

K,   Diehl stability coefficient.

k,   Munk's biplane span factor.

$A = \frac{(kb)^2}{S}$,   effective aspect ratio.

b,   span, ft.

τ,   correction for plan-form shape, τ_o for an
          elliptical plan form.

i_w,   angle of wing setting, degrees.

i_t,   angle of tail setting, degrees.

α,   angle of attack referred to airfoil chord, degrees.

α_T,   angle of attack referred to thrust line.

α_a,   absolute angle of attack, measured from the line of motion when the lift force is zero.

α_{L_0},   angle of attack for zero lift.

φ,   angle between the line joining the c.g. and the point 0.24c and the line perpendicular to the chord line of the wing, in a counterclockwise direction, degrees. *when viewed from which side, and counterclockwise from which line?*

φ_a,   the angle φ referred to the zero-lift direction instead of to the chord.

ϵ,   angle of downwash, degrees.

θ,   angle of pitch, degrees.

INTRODUCTION

The longitudinal stability of airplanes has become increasingly important as air-passenger traffic has grown. The trend of design toward low-wing monoplanes with their inherent stability problems has also brought about added study along these lines.

One of the most important factors in the analysis of the longitudinal stability is the derivative of the pitching moment due to an angular increment of pitch, expressed as $dM/d\theta$, or $dM/d\alpha$. Lieutenant Commander Walter S. Diehl of the Bureau of Aeronautics, Navy Department, developed a system of static-stability analysis which has proved quite satisfactory. The stability characteristics were determined in flight for several naval airplanes with regard to whether they were stable or unstable. A coefficient K was determined for each of these airplanes from the relationship $\dfrac{dM}{d\alpha} = KqWc$ or $\dfrac{dC_m}{d\alpha} = K\dfrac{W}{S}$ using the results of wind-tunnel tests on models of the respective

airplanes for $\frac{dM}{d\alpha}$. It was found that values of K for satisfactory longitudinal stability range from -0.0004 to -0.0008.

This paper develops an analysis concerning the factors governing the term $dM/d\alpha$ somewhat along the method used by Diehl but with the addition of certain original modifications and amplifications to generalize the problem for application to all types of airplanes in a manner suitable for the aircraft designer.

THE PITCHING MOMENT OF AN AIRPLANE

All parts of an airplane exposed to the air experience pressures that total to produce the resultant pitching moment of the airplane. Most of these components are small and are relatively unimportant in the study of longitudinal stability. Conversely, the pitching moments of the wing proper and of the horizontal tail are very important and determine practically alone the stability characteristics of the airplane.

An analysis of the forces on the various parts under different conditions of flight shows that for most conventional wing and fuselage arrangements the important forces are the wing lift, the wing induced drag, and the lift from the horizontal tail. For this analysis all other moment-producing forces have therefore been neglected in order to simplify the relationships. The order of magnitude of the discrepancies may be seen by the comparison with data obtained from wind-tunnel tests and from airplanes in flight.

Figure 1 shows a diagram of the vectors of the wing lift and wing induced drag in relation to the mean aerodynamic wing and the center of gravity of the airplane. In this figure, the center of gravity is shown both for a high and a low wing position, the symbols being differentiated by subscripts $_1$ and $_2$, respectively. The point $0.24c$ refers to the point 24 percent of the chord from the leading edge on the mean aerodynamic chord, about which point the wing pitching moment is practically constant. This point is frequently called the aerodynamic center (reference 1). The ratio d/c represents the distance in fractions of the chord from the center of gravity to the point $0.24c$.

Using the symbols previously listed, one may write from figure 1

$$M_{c.g.} = L_W \, t + D_p - L_t \, l \, \eta \quad \text{(moment of tail)}$$

$$= \left(L_W \, r + Dm \right) + L_W \, d \, \sin(\varphi - \alpha) +$$

$$Dd \, \cos(\varphi - \alpha) - L_t \, l \, \eta$$

$$= \left(M_{0.24c} \right) + d \left[L_W \, \sin(\varphi - \alpha) + D \, \cos(\varphi - a) \right] -$$

$$L_t \, l \, \eta$$

$$C_{m_{c.g.}} = C_{m_{0.24c}} + \frac{d}{c} \left[C_{L_W} \sin(\varphi - \alpha) + C_D \cos(\varphi - \alpha) \right] -$$

$$C_{L_t} \frac{S_t}{S_W} \frac{l}{c} \eta \qquad (1)$$

But

$$C_D = C_{D_o} + C_{D_i} = C_{D_o} + \frac{C_{L_W}^2 \, S_W}{\pi (kb)^2}$$

as previously mentioned, the effect of the moments due to the profile and parasite drags may be neglected in most cases, hence

$$C_D = \frac{C_{L_W}^2 \, S_W}{\pi (kb)^2} = \frac{C_{L_W}^2}{\pi \, A_W} \qquad (2)$$

and

$$C_{m_{c.g.}} = C_{m_{0.24c}} + \frac{d}{c} \left[C_{L_W} \sin(\varphi - \alpha) + \frac{C_{L_W}^2}{\pi \, A_W} \cos(\varphi - \alpha) \right] -$$

$$C_{L_t} \frac{S_t}{S_W} \frac{l}{c} \eta \qquad (3)$$

$$C_{m_{c.g.}} = C_{m_{0.24c}} + \frac{d}{c} \left[\frac{dC_{L_W}}{d\alpha} \alpha_a \sin(\varphi - \alpha) + \right.$$

$$\left. \left(\frac{dC_{L_W}}{d\alpha} \right)^2 \frac{\alpha_a^2}{\pi \, A_W} \cos(\varphi - \alpha) \right] - \frac{dC_{L_t}}{d\alpha} \times$$

$$\frac{S_t}{S_W} \frac{l}{c} \eta \left[\alpha_a + \alpha_{L_o} - i_W + i_t - \frac{36}{A_W} \frac{dC_{L_W}}{d\alpha} \alpha_a \right] \qquad (4)$$

where

$$\frac{dC_{L_W}}{d\alpha} = \frac{0.1015}{1 + \frac{1.85}{A_W}(1 + \tau_W)} \quad\text{and}\quad \frac{dC_{L_t}}{d\alpha} = \frac{0.1015}{1 + \frac{1.85}{A_t}(1 + \tau_t)}$$

$$\epsilon = \frac{36}{A_W} C_{L_W}, \quad \text{an approximate average.}$$

$$\alpha_t = \alpha_W - i_W + i_t - \epsilon \tag{5}$$

$$= \alpha_a + \alpha_{L_o} - i_W + i_t - \epsilon \quad (\text{see fig. 2}) \tag{6}$$

By means of the foregoing expression, the pitching-moment coefficient for an airplane may be readily computed. In order to facilitate this computation, nomographic charts (figs. 3 and 4) have been prepared. These charts appear complex due to the number of variables involved, but may be easily followed. Values of $C_{m_{0.24c}}$ (for practical purposes equal to C_{m_0}) may be found in various N.A.C.A. reports or may be derived from the following empirical formula (see reference 2):

$$C_{m_{0.24c}} = \left[1.10 + 3.8\left(\frac{x}{c} - \frac{t}{c}\right)\right]\frac{m}{c} \tag{7}$$

where $\frac{x}{c}$ = distance from leading edge to ordinate of maximum camber, in fractions of the chord.

$\frac{t}{c}$ = thickness, in fractions of chord.

$\frac{m}{c}$ = camber, in fractions of the chord.

The successive increments of the total pitching-moment coefficients are added together to obtain the final pitching-moment coefficient about the center of gravity, or

$$C_{m_{c.g.}} = C_{m_{0.24c}} + C_{m_{L_W}} + C_{m_{D_i}} - C_{m_t} \cdot \cdot \tag{8}$$

THE EQUATION FOR LONGITUDINAL STATIC STABILITY

The principal requirement for longitudinal static
stability is that the curve of the pitching moment (or
pitching-moment coefficient) of the airplane when plotted
on the basis of angle of attack should be smooth, have a
negative slope throughout and have an angle of trim (zero
moment, the condition of equilibrium) within the flight
range. The position of the angle of trim may be obtained
by a suitable value of the tail-plane setting. In gener-
al most airplanes have regular, smooth curves but not all
have the requirement of a satisfactory negative slope.
Over a period of years the Navy Department has been ob-
taining data on airplanes in flight and comparing their
stability with the slope of their respective pitching-
moment curves obtained from data on models. This work
has been reported by Diehl who developed an empirical re-
lation for the same. (See reference 3.) This relation
is expressed as follows:

$$\frac{dM}{d\alpha} = K \, q \, W \, c$$

or
$$\frac{dC_m}{d\alpha} = K \frac{W}{S} \qquad\qquad (9)$$

Diehl found values of K for satisfactory stability con-
ditions to be as given in table I. From the values for
the naval airplanes, the values for the commercial types
have been deduced. Values less numerically than -0.0004
should be considered too low and those greater numerical-
ly than -0.0010 too high; the one produces too weak a re-
sponse and the other would be a trifle too stiff for hand-
ling. Positive values, of course, indicate instability
and should be avoided entirely.

TABLE I

STABILITY COEFFICIENT, K

Type of airplane	K sq.ft./lb./deg.
Fighter	−0.00040
Observation	−−.00060
Bomber	−.00080
Sport, Racer	−.00040
Private, General purpose, Mail	−.00060
Commercial transport, small	−.00060
" " , large	−.00080

In order to obtain a value of K, the stability co-efficient, for a particular airplane it is first neces-sary to reduce equation (4) for the pitching-moment coef-ficient to its first derivative with respect to α, which is then an expression for its slope at any point. This result can then be equated to $K\frac{W}{S_W}$ as given in equation (9). After expansion and obtaining the derivative, the important first-order terms were retained giving the fol-lowing result:

$$\frac{dC_{m_{c.g.}}}{d\alpha_a} = \frac{d}{c}\left[\sin\varphi_a \left\{ \frac{dC_{L_W}}{d\alpha}(1 - 0.000456\,\alpha_a^2) + \right.\right.$$

$$0.01667\left(\frac{dC_{L_W}}{d\alpha}\right)^2 \frac{\alpha_a^2}{A_W}\right\} - \cos\varphi_a$$

$$\left\{\frac{dC_{L_W}}{d\alpha}(0.0349\,\alpha_a - 0.00000354\,\alpha_a^3) - \right.$$

$$0.636\left(\frac{dC_{L_W}}{d\alpha}\right)^2 \frac{\alpha_a}{A_W}\right\}\right] - \frac{dC_{L_t}}{d\alpha}\frac{S_t}{S_W}\frac{l}{c}\eta\left[1 - \frac{36}{A_W}\frac{dC_{L_W}}{d\alpha}\right] \quad (10)$$

$$\frac{dC_{m_{c.g.}}}{d\alpha_a} = \frac{d}{c} \left[\sin \varphi_a \, F_1 - \cos \varphi_a \, F_2 \right] - F_3 \frac{dC_{L_t}}{d\alpha} \frac{S_t}{S_W} \frac{l}{c} \eta \qquad (11)$$

where

$$F_1 = \left\{ \frac{dC_{L_W}}{d\alpha} \left(1 - 0.000456 \, \alpha_a{}^2 \right) + 0.01667 \left(\frac{dC_{L_W}}{d\alpha} \right)^2 \frac{\alpha_a{}^2}{A_W} \right\} \qquad (12)$$

$$F_2 = \left\{ \frac{dC_{L_W}}{d\alpha} \left(0.0349 \, \alpha_a - 0.00000354 \, \alpha_a{}^3 \right) - \right.$$
$$\left. 0.636 \left(\frac{dC_{L_W}}{d\alpha} \right)^2 \frac{\alpha_a}{A_W} \right\} \qquad (13)$$

$$F_3 = \left[1 - \frac{36}{A_W} \frac{dC_{L_W}}{d\alpha} \right] \qquad (14)$$

Charts of values of F_1, of F_2, and of F_3 and $\frac{dC_L}{d\alpha}$ will be found in figures 5, 6, and 7, respectively. With given specifications for an airplane, a solution for the stability coefficient may be readily found for any desired angle of attack.

DISCUSSION

When biplanes were the usual type of design, it usually happened that the center of gravity was located very close to or on the mean aerodynamic chord. The pitching moment against angle-of-attack curves obtained from wind-tunnel tests for this condition were nearly always approximately straight lines. This result led to the assumption that all such moment curves might be similar. The subject was vague at best and not of sufficient importance to demand more than simple flight tests to check the stability, as the type was practically sure to be at least stable. But with the commercial aspect becoming more and more important and the monoplane becoming the common type, more attention to the static stability is necessary before the manufacturer can go into production. Quite satisfactory results may be obtained by a study of the important factors; horizontal center-of-gravity position, vertical center-of-gravity position, tail size and position, interferences, and other variables.

Effect of Horizontal c.g. Position

As the c.g. position is varied fore and aft with respect to the wing chord, the pitching-moment coefficient against angle-of-attack curve increases or decreases its slope rotating about a value of the condition when the lift force is zero. The exact values obtained, of course, are functions of the geometry of the particular airplane. It is well known that satisfactory stability usually occurs when the center of gravity is located between 25 and 30 percent of the chord from the leading edge. Figure 8 shows this effect for a typical airplane.

Effect of Vertical c.g. Position

The vertical position of the center of gravity is very important particularly in that on the prevailing monoplanes of low-wing type it tends to increase the stability problems. In this development for the pitching-moment coefficient, the vertical as well as the horizontal location of the center of gravity is considered as shown by the derived expression. When the c.g. is above the chord the pitching-moment coefficient (against α) curve is not a straight line but is a curve concave upward. When the c.g. is below, the curve is concave downward. The two types bend away from each other as the angle of attack increases. Figure 9 is a chart illustrating these effects for monoplanes of different wing locations.

Figure 10 is a vector diagram for a monoplane, on which are plotted the c.g. for a parasol arrangement and the c.g. for a low-wing arrangement. In the former case the pencil of resultant force vectors points above the c.g. with an increasing moment arm from the c.g. to the force vector as the angle of attack is increased. For the high c.g. the vectors point below and produce decreasing moment arms as the angle increases. In the first case an increasing slope to the moment curve is produced, and in the second case a decreasing slope.

It is then evident that the stability characteristics of the low-wing monoplane are decidedly different from the high-wing or parasol type. Given two airplanes of like characteristics at high speed, the low-wing airplane with its high c.g. would be the less stable and the high-wing

airplane would be too stable at low speeds. In neither case can the same degree of stability be obtained for both the high- and low-speed conditions.

Using the Diehl stability coefficient K and assuming like tail-plane areas and effects, figure 11 has been drawn to illustrate the relation between the location of the c.g. and K. Here are shown lines of equal values of K; one set for high speed ($\alpha = 0^{\circ}$) and one set for low speed ($\alpha = 20^{\circ}$). Satisfactory values are indicated. In order to be within the desirable range, the location of the c.g. is limited to a small diamond-shaped area just aft of the point 0.24c on the chord line. A heavy line is shown on which the c.g. might be placed and where equal values of K for low and for high speed might be obtained; with a mid-wing monoplane or a biplane this could be done, but it is impracticable with other types. Figure 11 may also be used to obtain rough preliminary stability information by correcting for the tail plane as indicated.

Effect of Variables A_w, A_t, $\frac{S_t}{S_w}$, $\frac{l}{c}$, and η

In figure 12, graphs are given showing the effect of the other variables of the stability equation, A_w, A_t, $\frac{S_t}{S_w}$, $\frac{l}{c}$, and η. An increase in the "effective" aspect ratio of the wing (A_w) improves the stability in an indirect manner, principally through reduction of the downwash on the tail plane. With an increase of A_w the value of K therefore increases more rapidly, however, for a high-wing than for a low-wing monoplane. The change of K with angle of attack or speed is also indicated in this figure. The efficiency of the high wing is again evident.

The remaining variables bear straight-line relationships with K and may be considered together as functions of certain basic values. Figure 12 also shows the effects of tail efficiency η, effective tail aspect ratio A_t, as well as of ratios S_t/S_w, and lever arm in terms of the chord, l/c. Different scales for each variable make it possible to use single curves and show at once the relative change in K due to a modification in the tail and its efficiency. The geometry of the tail may be readily changed by the designer to fit his requirements; the tail efficiency, however, is not so easily mod-

ified and necessitates a detailed study of the wing, fuselage, and motor interferences. A tail efficiency of 70 to 80 percent is an average value for the present-day type of monoplane. An efficiency of 80 to 90 percent is probable of attainment where extreme care is taken in filleting, cowling, and by the smooth fairing of the fuselage. A large aspect ratio of the tail is also beneficial as it removes the effective area from the fuselage and its detrimental interference. Thin wings materially aid in reducing the turbulence troubles of fuselage-wing interference.

Effect of Fillets and Burbling

In recent wind-tunnel testing on airplane models, it has been noticed that irregularities in the curves of the pitching-moment coefficient (C_m against α) for low-wing monoplanes occur in the region of the stall. In two or three cases this irregularity, or hump, in the curve proved a very unsatisfactory condition which had to be eliminated. The addition of larger fillets between the thick monoplane wing and the fuselage only aggravated the difficulty. Smaller fillets and an enlarged tail area aided materially.

From an analysis of the effect of the wing lift in the moment equation, it may be seen that at the stall, or burble point, the decrease in lift reduces the positive moment and allows the beneficial negative moment of the tail to govern. This effect increases the negative slope of the tail thereby greatly aiding the stability. The curves labeled a in figure 13 show the lift coefficient C_L, pitching-moment coefficient C_m, and stability coefficient K for a hypothetical low-wing airplane, curves b, a low-wing airplane with burbling effects, and curve c, a low-wing airplane with fuselage interferences in addition. The hump previously mentioned is evident. The unfilleted wing-fuselage arrangement produces a far better shaped curve. As filleting is added the curves tend to approach the curves b, and, as burbling is prevented, a bad hump is developed. It is well known that filleting tends to prevent buffeting, yet the designer should assure himself that the stability is ample in the region of the stall.

Effect of Loading

The large commercial transports often have a big range of horizontal center-of-gravity position between the fully loaded condition and the empty condition, as when ferrying. A change of 10 percent from 0.34 M.A.C. to 0.24 M.A.C. is common. This condition makes it difficult to obtain satisfactory stability characteristics at all angles of attack. Figure 8 is a chart giving a series of curves of C_m and K representing values for a low-wing monoplane with the c.g. at 0.34 M.A.C. and at 0.24 M.A.C. and with three tail areas. It is shown in this figure that considerable difficulty will be encountered and it would often be advisable to carry lead weights to maintain a more reasonable weight distribution in the unloaded condition.

Comparison with Tests

Several sets of data from tests on airplane models in the wind tunnel (University of Detroit 7- by 10-foot wind tunnel) were available and have been used to compare and judge the general accuracy of the basic assumptions and the final form of the above-derived equations of the pitching-moment and the stability coefficients. Four typical designs have been chosen: a high-wing cabin monoplane, an open cockpit parasol monoplane, a small low-wing airplane, and a large commercial low-wing transport.

Figure 14 gives the pitching-moment coefficient against absolute angle of attack of a four-place high-wing cabin monoplane. A pitching-moment curve computed from the equation is included for comparison. The agreement between the test curve and that computed is very good. After the burble the test values drop away as expected. The stability characteristics of this airplane are quite satisfactory and agree with the values derived from the equation.

Figure 15 gives a similar comparison for a parasol monoplane. In the computation of the pitching moment a tail efficiency of 80 percent was chosen. Had 78 percent been used, the computed pitching-moment coefficient curve would have agreed ideally with the wind-tunnel test data.

In the first comparisons, high-wing arrangements were used whereas figures 16 and 17 show curves for low-wing types. Figure 16 contains the data for a small cabin airplane. The change in the general shape of the curves is to be noted, typical of the low-wing position. The agreement here is also very satisfactory both for C_m and for K.

Figure 17 is for a large high-speed passenger transport. Test values for K agree very closely with the computed values. The C_m curve as computed, however, is displaced vertically from the test-value curve. This vertical shift represents a variation in tail setting of approximately $0.4°$, a possible and unimportant error in model construction.

From tests on a Fairchild F-22 airplane by the N.A.C.A. (reference 4), values of C_m for that airplane are given in figure 18. Computed values show good agreement of stability coefficient as the shapes of the two curves for K are similar. With a change in tail setting or wing incidence of approximately $1.6°$, the C_m curves would also agree.

General

The effect of lengthening the tail lever arm is especially beneficial to the stability of an airplane. The general expression for the damping in pitch,

$$\frac{dM}{d\Omega} = \frac{dC_{L_t}}{d\alpha} \frac{1}{2} \rho V S_t l^2$$

(where Ω is the angular velocity in pitch) gives the second power of the variable l. The criterion of static stability $\frac{dC_{m_{c.g.}}}{d\alpha}$ has it as the first power. Any increase in the tail length then not only increases the static stability considerably but increases the dynamic stability still more, a point not to be neglected. The structural difficulties, however, must also be considered.

These two expressions for $C_{m_{c.g.}}$ and K, or $\frac{dC_{m_{c.g.}}}{d\alpha}$ make it possible readily to estimate and compute

values of the pitching-moment coefficient, find the angle of trim, and determine the stability characteristics for various types of airplanes with satisfactory accuracy to insure good full-scale results. Certain assumptions in regard to drag effects have been made but, in light of the agreement obtained with experimental data, it is felt that these assumptions have been justified.

It is important to note that the $C_{m_{0.24c}}$ has disappeared from the expression for the stability coefficient. This disappearance is, of course, due to the fact that the wing moment about that point is constant and does not change with the angle of attack. The stability of the airplane is <u>independent</u> of the pitching-moment characteristics of the wing.

CONCLUSIONS

This study on the longitudinal stability of the present-day airplane has developed expressions for the pitching-moment coefficient and the static stability that may be used with confidence by airplane designers.

The distinctive type of the pitching-moment curves for the high-wing and low-wing monoplane makes the stability treatment of each a separate problem. The dimensional characteristics required for stability of the high-wing monoplane are determined by the minimum allowable at angles of attack corresponding to high speed and the increasing stiffness of the controls as the angle of attack approaches the stall. The low-wing monoplane, however, may be unstable at high angles of attack if the dimensional characteristics are such as to give satisfactory stability at low angles.

The effect of burbling of the flow is, in general, beneficial to the stability, tending to make the airplane controls stiff beyond the stall.

Filleting as used on low-wing monoplanes is detrimental to stability, but this effect can be overcome by other means.

The stability of the airplane is found to be independent of the pitching-moment characteristics of wings of conventional type.

REFERENCES

1. Munk, Max M.: Computation of Longitudinal Stability.
      Aero Digest, October 1933.

2. Wood, Karl D.: Technical Aerodynamics. College of En-
      gineering, Cornell University, Ithaca, N.Y., 1933.

3. Diehl, Walter S.: Engineering Aerodynamics. The Ron-
      ald Press Co., 1928.

4. Wallace, Rudolf N.: The Effect of Split Trailing-Edge
      Wing Flaps on the Aerodynamic Characteristics of a
      Parasol Monoplane. T.N. No. 475, N.A.C.A., 1933.

BIBLIOGRAPHY

Higgins, George J.: The Prediction of Airfoil Character-
      istics. T.R. No. 312, N.A.C.A., 1929.

Jacobs, Eastman N., Ward, Kenneth E., and Pinkerton, Rob-
      ert M.: The Characteristics of 78 Related Airfoil
      Sections from Tests in the Variable-Density Wind Tun-
      nel. T.R. No. 460, N.A.C.A., 1933.

Klein, A. L.: The Effect of Fillets on Wing-Fuselage In-
      terference. Trans. A.S.M.E., vol. 56, no. I, January
      1934, pp, 1-10.

Stalker, Edward Archibald: Principles of Flight. The
      Ronald Press Co., 1931.

Warner, Edward P.: Airplane Design - Aerodynamics.
      McGraw-Hill Book Co., Inc., 1927.

$$\alpha_w = i_w - i_t + \alpha_t + \epsilon.$$

$$\alpha_t = \alpha_w - i_w + i_t - \epsilon.$$
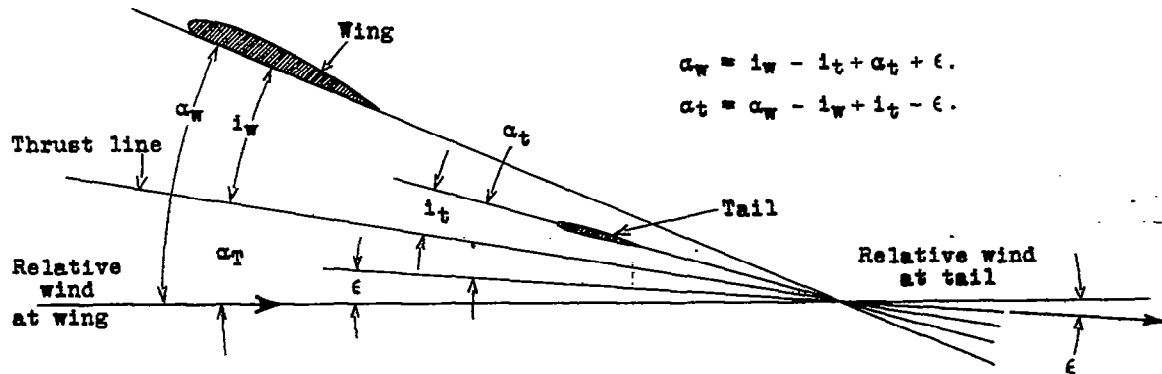
Figure 2.- Angular relation of wing and tail.
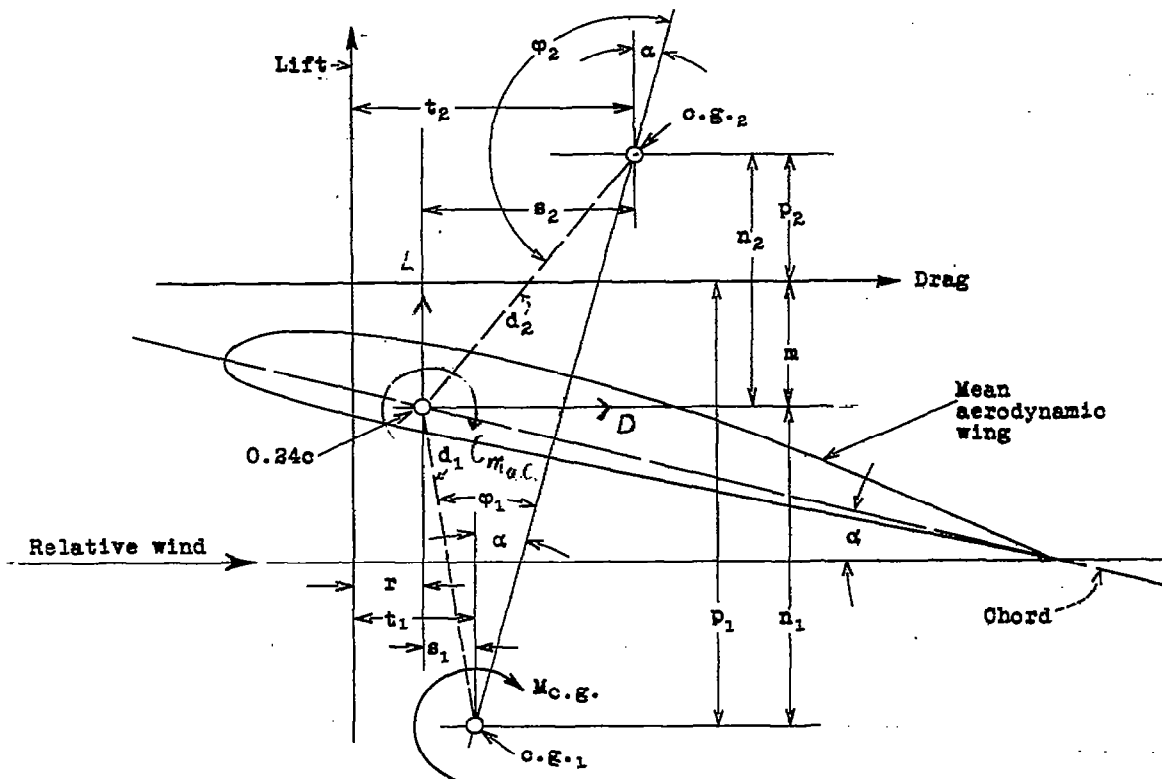
Figure 1.- Pitching-moment diagram of low-wing or high-wing monoplane.
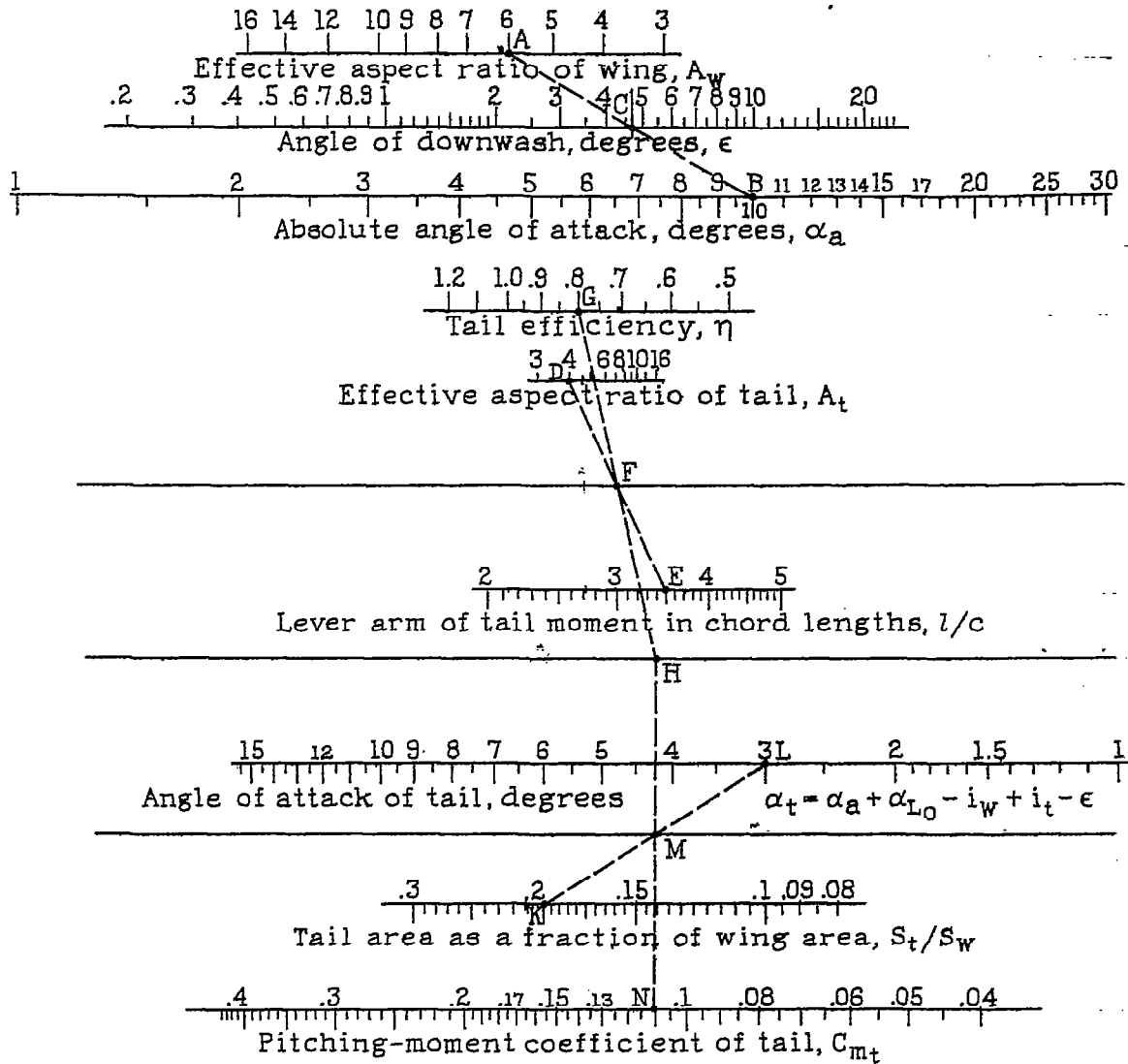
$$C_{m_t} = \frac{0.1015}{1 + \dfrac{1.85}{A_t}} \frac{l}{c} \frac{S_t}{S_w} \eta \left[\alpha_a + \alpha_{L_0} - i_w + i_t - \frac{36}{A_w} \frac{0.1015}{1 + \dfrac{1.85}{A_w}} \alpha_a \right]$$

Legend	
A — B = C	G — F = H
D — E = F	K — L = M
	H — M = N Answer

Figure 3. — Nomograph for determining the pitching-moment coefficient due to the tail.

$$C_{m_{L_W}} = \frac{d}{c} \frac{dC}{d\alpha} \alpha_a \sin(\varphi_a - \alpha_a)$$

Degrees, $(\varphi_a - \alpha_a)$

d/c

Effective aspect ratio of wing, A_W

Absolute angle of attack, degrees, α_a

Pitching-moment coefficient due to lift on wing, $C_{m_{L_W}}$

Degrees, $(\varphi_a - \alpha_a)$

Legend
A — B = C
D — E = F
F — C = G Answer

d/c

Effective aspect ratio of wing, A_W

Absolute angle of attack, degrees, α_a

Pitching-moment coefficient due to induced drag on wing, $C_{m_{D_i}}$

$$C_{m_{D_i}} = \frac{d}{c} \left[\frac{dC_L}{d\alpha}\right]^2 \frac{\alpha_a^2}{\pi A_W} \cos(\varphi_a - \alpha_a)$$
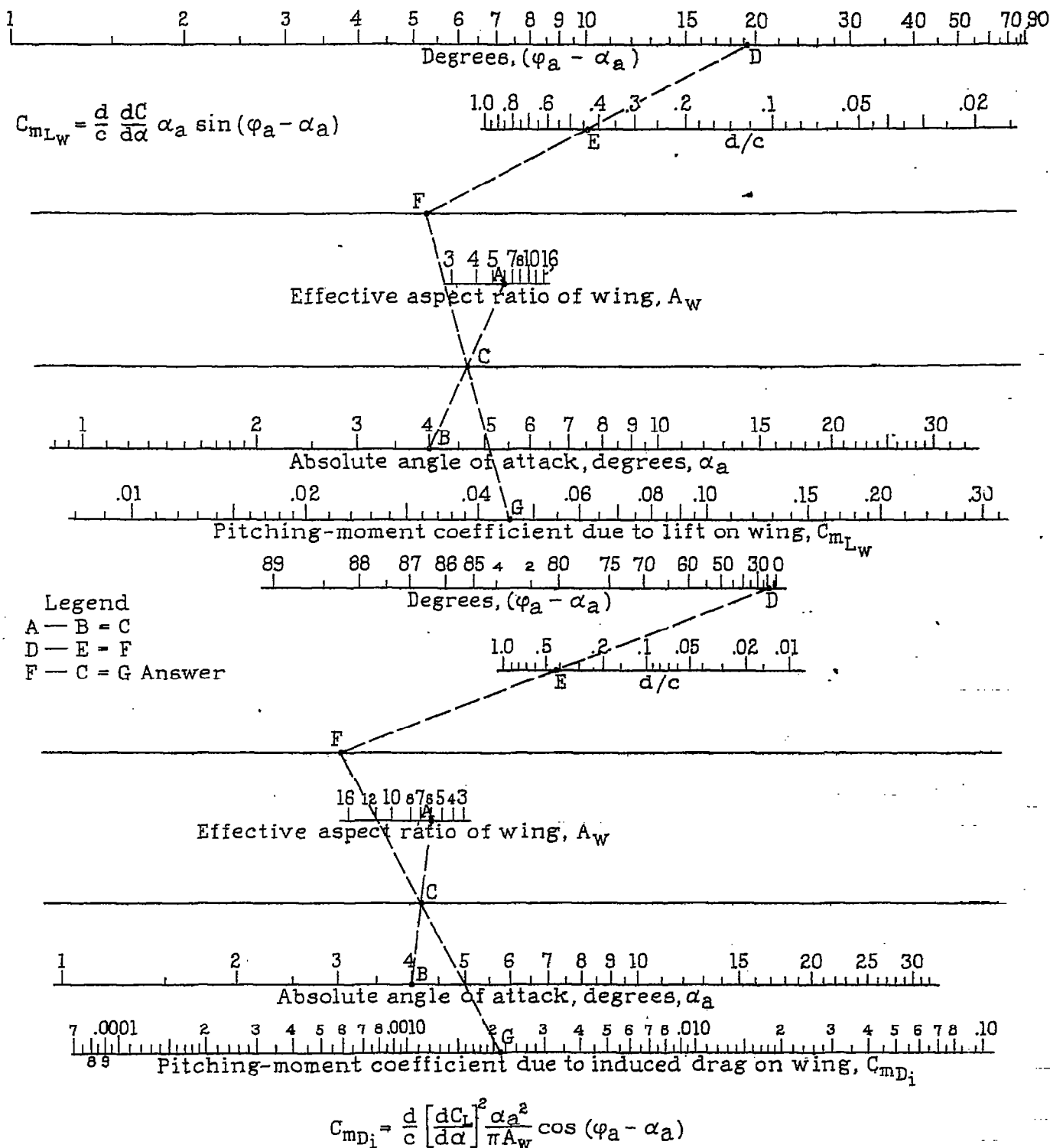
Figure 4. – Nomograph for determining the pitching-moment coefficient
due to the wing.
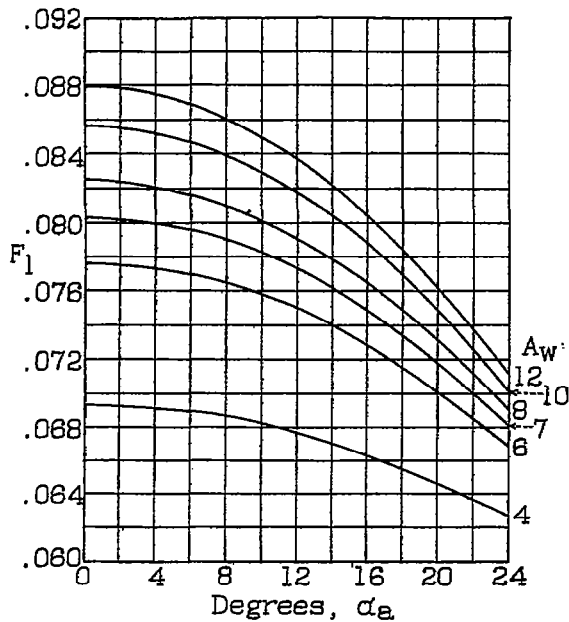
Figure 5.- Variation of factor F_1,
with absolute angle of
attack for different aspect ratios.
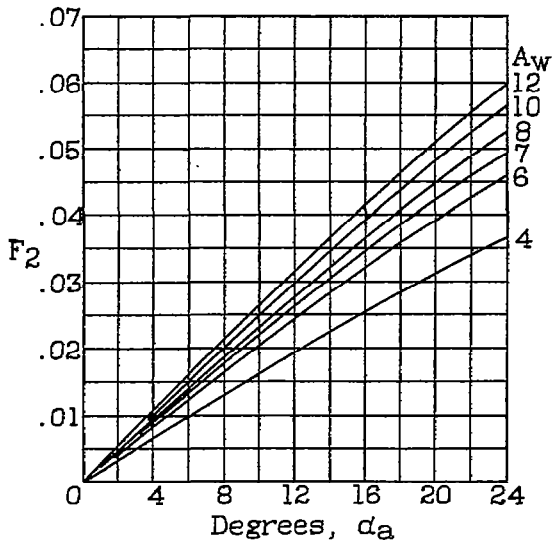
Figure 6.- Variation of factor F_2
with absolute angle of
attack for different aspect ratios.
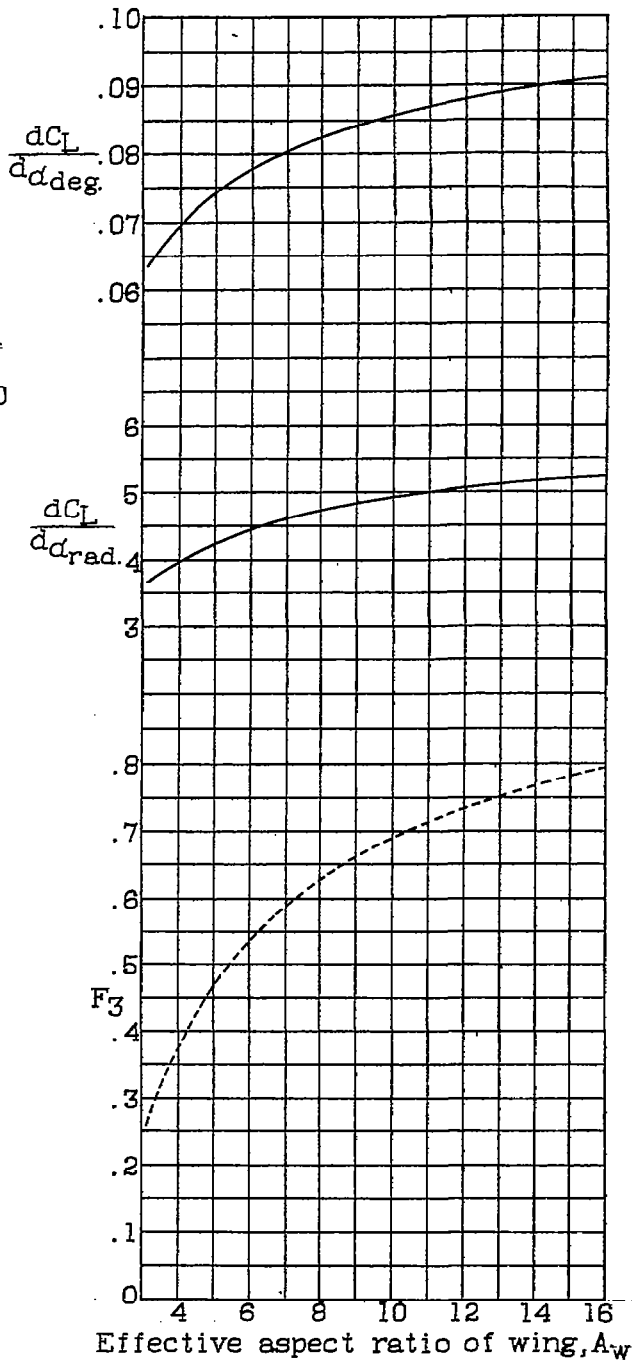
Figure 7.- Variation of factor F_3
and $dC_L/d\alpha$ with effec-
tive aspect ratio.
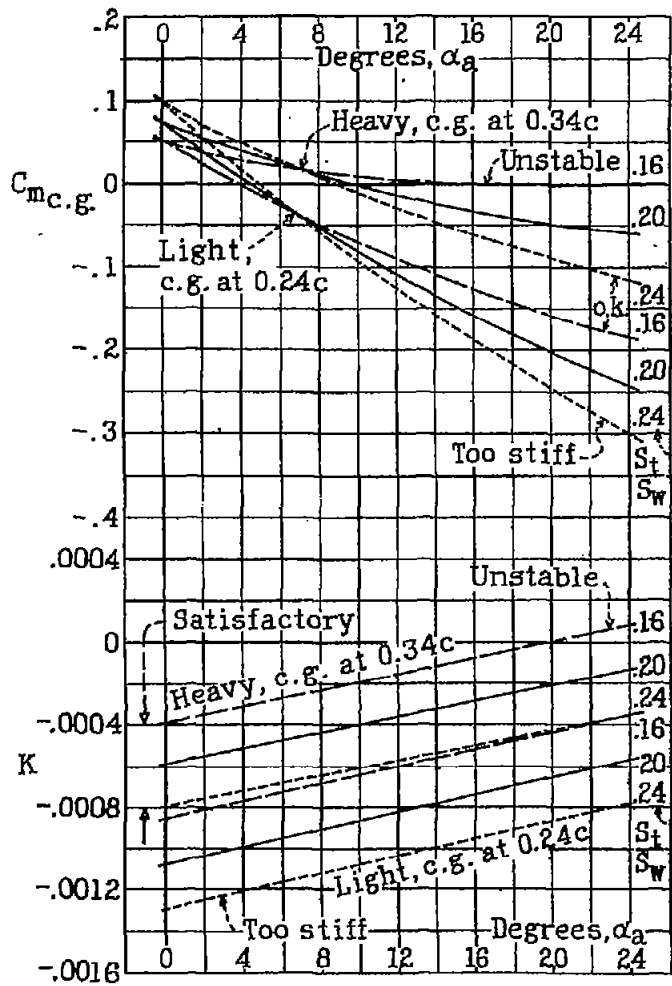
Figure 8.- The effect of horizontal position of the center of gravity on the stability coefficient. Light and heavy low-wing commercial airplanes.
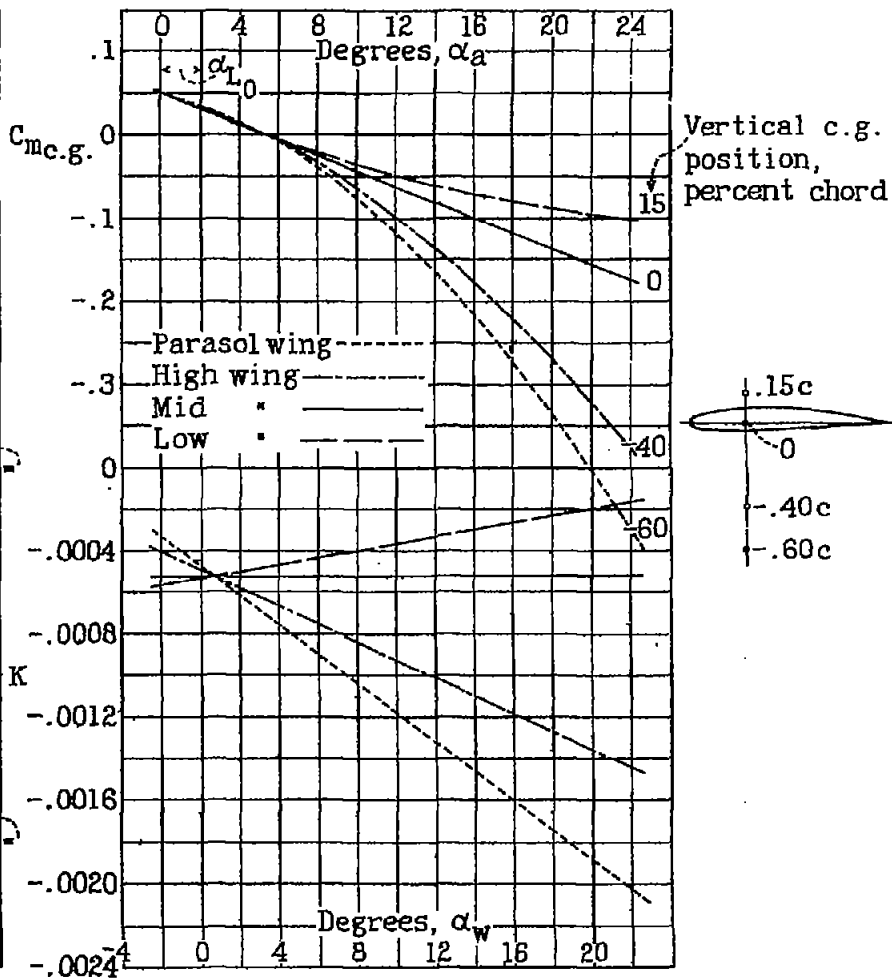
Figure 9.- The effect of vertical position of the center of gravity on the stability coefficient. Four types of commercial monoplanes.
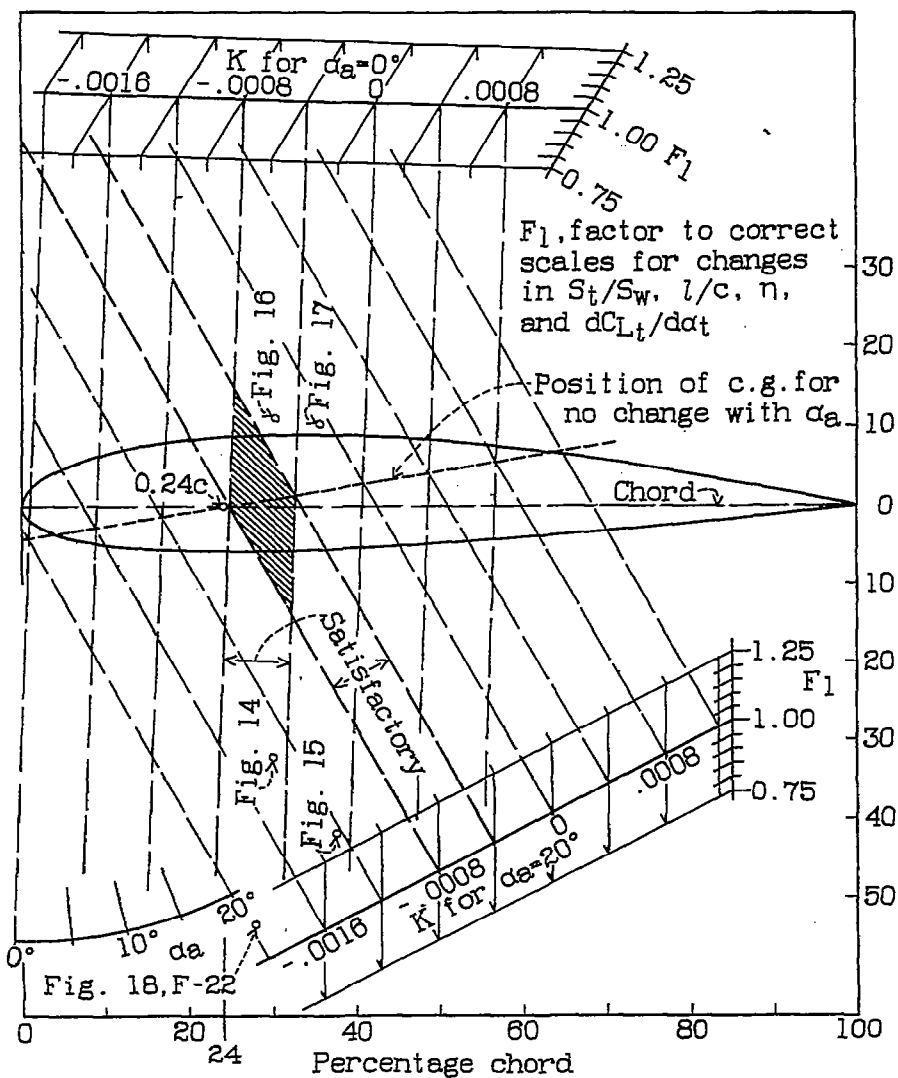
A_W	$= 7$
α_{L_O}	$= -2°$
i_w	$= 2°$
i_t	$= 0$
W/S	$= 18$
A_t	$= 3.75$
S_t/S_w	$= 0.16$
l/c	$= 3.00$
η	$= 0.70$
$C_{m_{0.24c}}$	$= -0.04$

Figure 11.- Effect of center-of-gravity location on the stability coefficient.
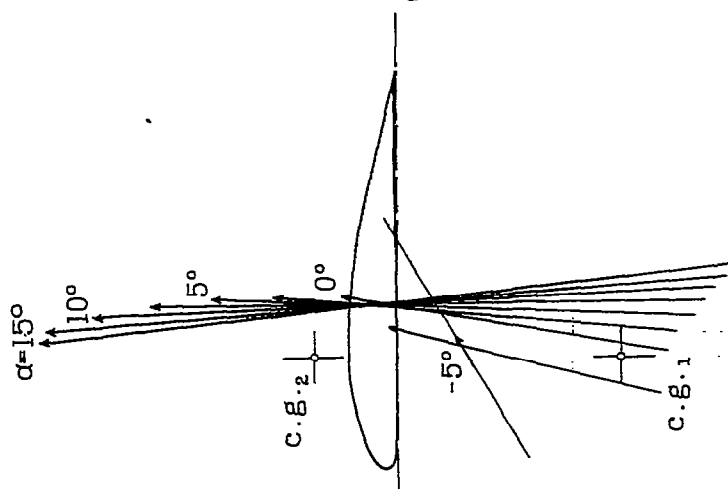
Figure 10.- Resultant force vectors for Fairchild F-22 parasol monoplane (see reference 4) and for a low-wing monoplane.
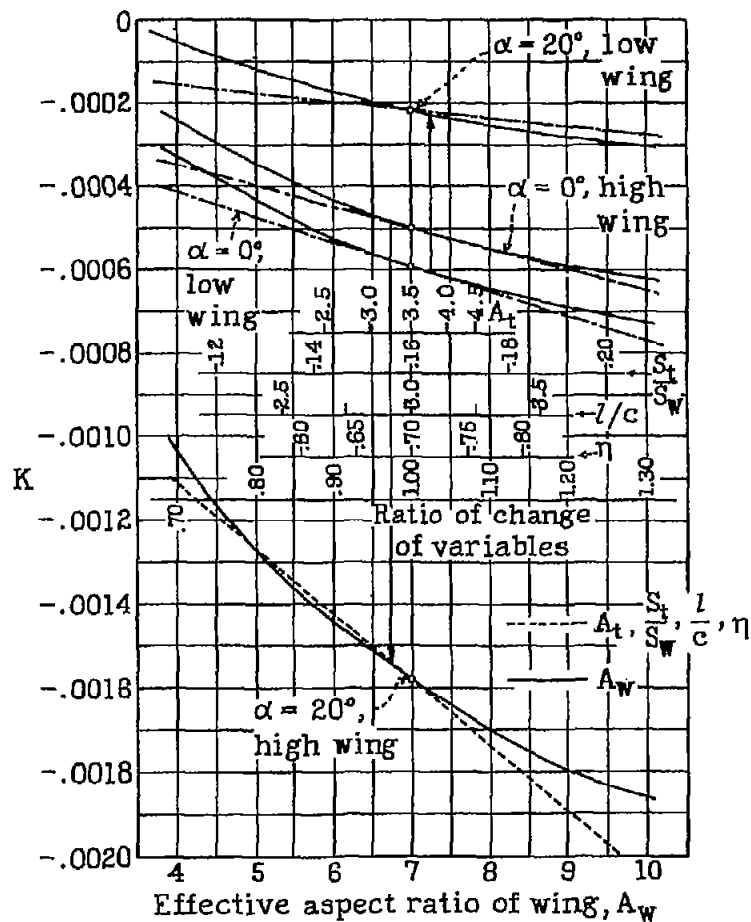
Figure 12.— Effect of different variables on the stability coefficient.

Figure 13.— The effect of filleting on the lift and pitching-moment coefficients of a low-wing monoplane.

a, hypothetical low-wing airplane.   b, low-wing airplane with burbling effects.
c, low-wing airplane with fuselage interference.
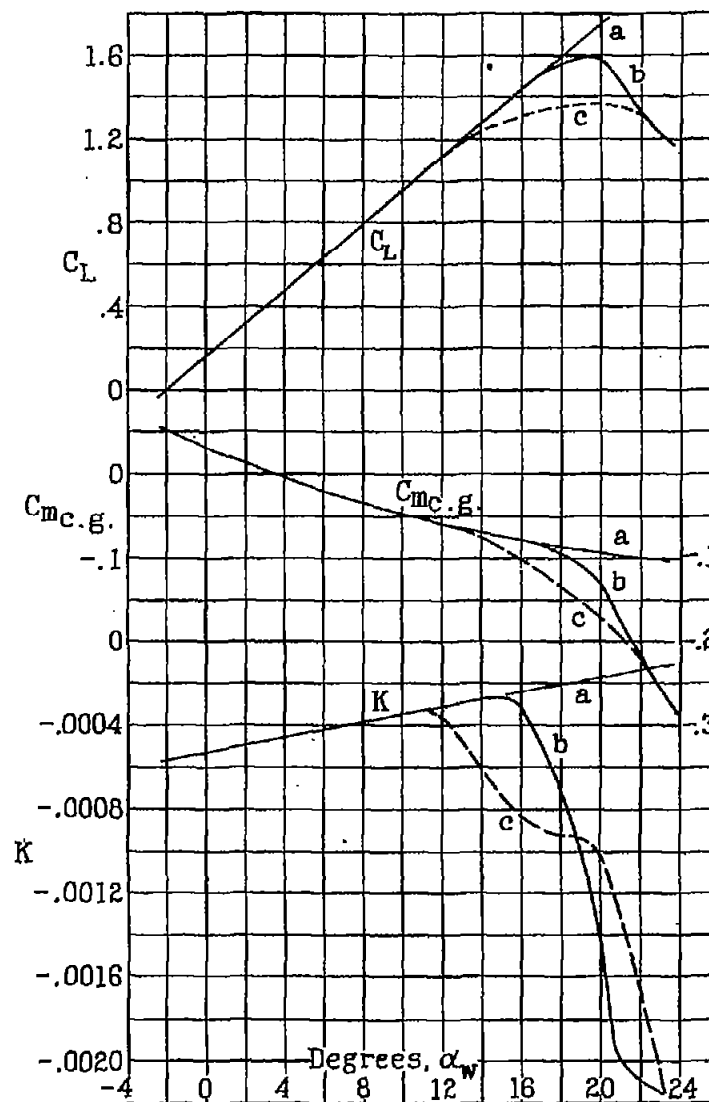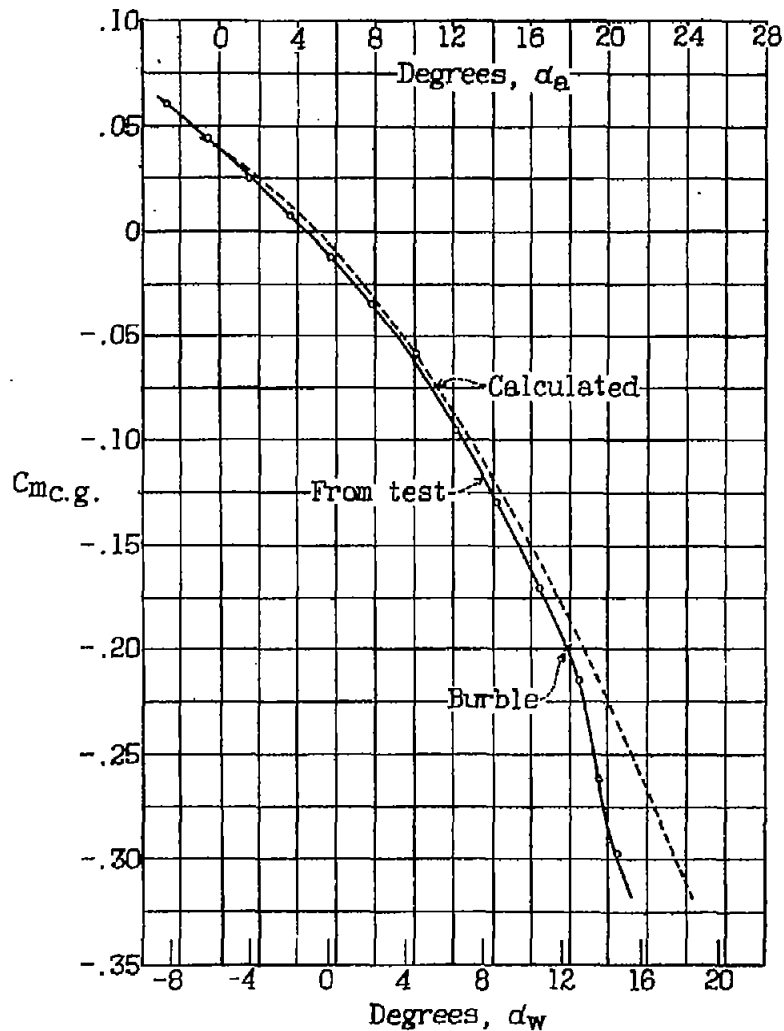
Figure 14.- Variation of pitching-moment
coefficient with absolute angle
of attack for a high-wing cabin monoplane.
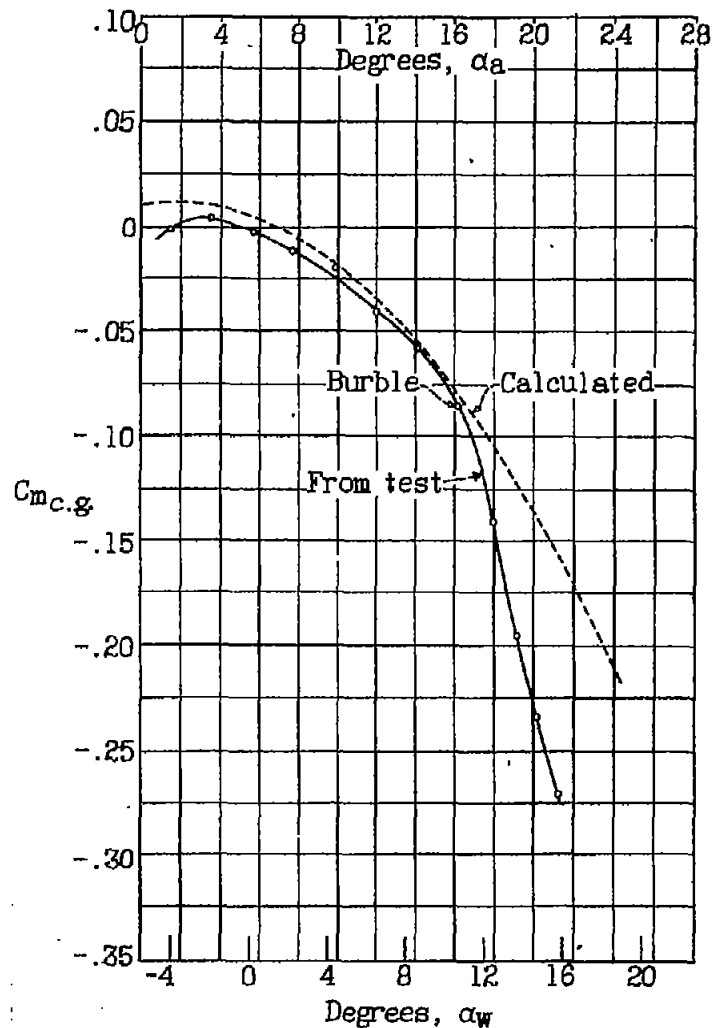University of Detroit 7 by 10 ft. wind tunnel.
1/6.25 size model.

Figure 15.- Variation of pitching-moment
coefficient with absolute angle
of attack for an open-cockpit parasol mono-
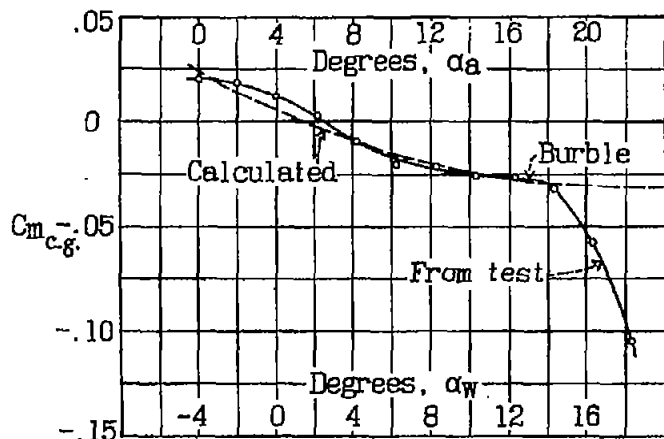plane. University of Detroit 7 by 10 ft. wind
tunnel. 1/8 size model.

Figure 16.- Variation of pitching-moment
coefficient with absolute angle
of attack for a small low-wing airplane.
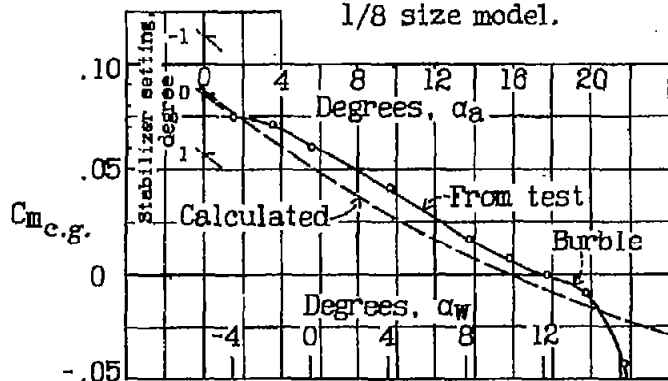University of Detroit 7 by 10 ft. wind-tunnel.
1/8 size model.

Figure 17.- Variation of pitching-moment
coefficient with absolute angle
of attack for a commercial low-wing transport.
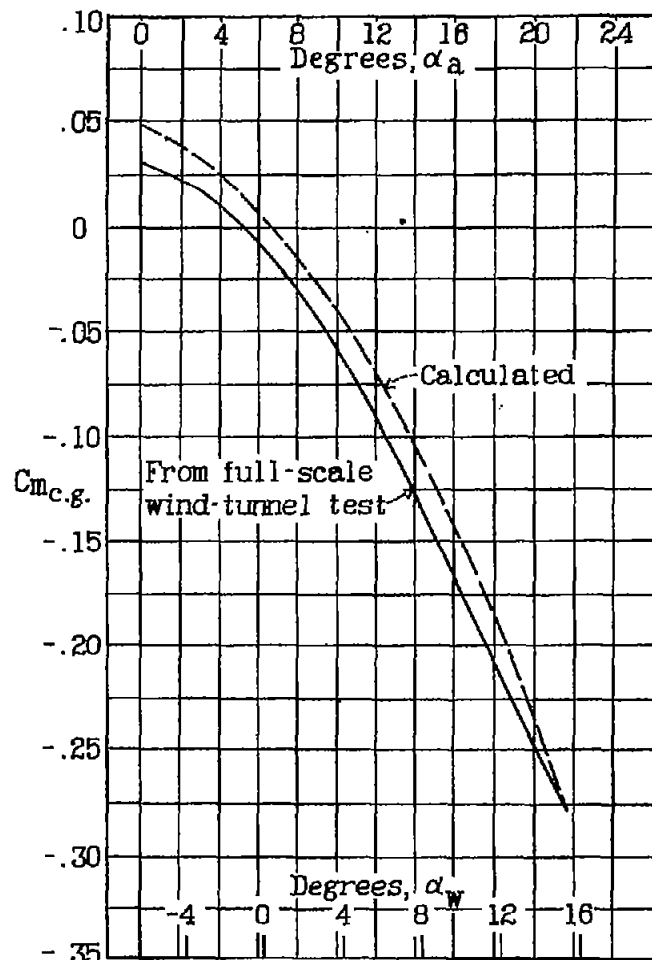University of Detroit 7 by 10 ft. wind-tunnel.
1/16 size model.

Figure 18.- Variation of pitching-moment
coefficient with absolute
angle of attack for a parasol monoplane.
N.A.C.A. full-scale wind tunnel.